

# Inconsistent blood brain barrier disruption by intraarterial mannitol in rabbits: implications for chemotherapy

Shailendra Joshi · Aysegul Ergin · Mei Wang ·  
Roberto Reif · Jane Zhang · Jeffrey N. Bruce ·  
Irving J. Bigio

Received: 27 April 2010 / Accepted: 8 November 2010  
© Springer Science+Business Media, LLC. 2010

**Abstract** The novel ability to quantify drug and tracer concentrations in vivo by optical means leads to the possibility of detecting and quantifying blood brain barrier (BBB) disruption in real-time by monitoring concentrations of chromophores such as Evan's Blue. In this study, experiments were conducted to assess the disruption of the BBB, by intraarterial injection of mannitol, in New Zealand white rabbits. Surgical preparation included: tracheotomy for mechanical ventilation, femoral and selective internal carotid artery (ICA) catheterizations, skull screws for monitoring electrocerebral activity, bilateral placement of laser Doppler probes and a small craniotomy for the placement of a fiber optic probe to determine tissue Evan's Blue dye concentrations. Evans Blue (6.5 mg/kg) was injected intravenously (IV) just before BBB disruption with intracarotid mannitol (25%, 8 ml/40 s). Brain tissue concentrations of the dye in mannitol-treated and control

animals were monitored using the method of optical pharmacokinetics (OP) during the subsequent 60 min. Hemodynamic parameters, heart rate, blood pressure, and EKG remained stable throughout the experiments in both the control and the mannitol-treated group. Brain tissue concentrations of Evan's Blue and the brain:plasma Evan's Blue partition coefficient progressively increased during the period of observation. A wide variation in brain tissue Evan's Blue concentrations was observed in the mannitol group. The experiments demonstrate the feasibility of measuring tissue concentrations of Evan's Blue without invading the brain parenchyma, and in real-time. The data suggest that there are significant variations in the degree and duration of BBB disruption induced with intraarterial mannitol. The ability to optically monitor the BBB disruption in real-time could provide a feedback control for hypertonic disruption and/or facilitate dosage control for chemotherapeutic drugs that require such disruption.

S. Joshi (✉) · M. Wang  
Department of Anesthesiology, PH 505, College of Physicians  
and Surgeons of Columbia University, 630 West 168th Street,  
New York, NY 10032, USA  
e-mail: sj121@columbia.edu

A. Ergin · R. Reif  
Department of Biomedical Engineering, Boston University,  
Boston, MA, USA

J. Zhang  
Boston University, Boston, MA, USA

J. N. Bruce  
Department of Neurosurgery, Columbia University, New York,  
NY, USA

I. J. Bigio  
Department of Biomedical Engineering, Electrical Engineering,  
and Physics, Boston University, Boston, MA, USA

**Keywords** Blood brain barrier disruption · Intraarterial · Mannitol

## Introduction

Safe, effective, and predictable disruption of the blood brain barrier (BBB) is a key step in the delivery of certain chemotherapeutic drugs, as well as nanoparticles, liposomes, and viral vectors—the current and future therapies for brain tumors and a range of other brain diseases [1]. BBB has been a major hurdle for the delivery of drugs to brain tissue [2]. The barrier seems to be far more complex and dynamic than perceived in the past. A variety of methods and drugs have been employed to disrupt the barrier and improve drug delivery [3–6]. However, for the last three decades

intraarterial mannitol has remained the main clinical method for transient disruption [7]. Limited clinical data from human subjects also shows that the degree of disruption, and subsequent concentrations of drugs in the cerebrospinal fluid, vary considerably after mannitol administration, Fig. 1 [8]. Many alternatives to mannitol have evolved over that time but none has found wide clinical application yet. Disruption of BBB with intracarotid mannitol is reasonably safe and its effectiveness is well supported by anecdotal evidence [9, 10]. Significant complications have also been reported during the procedure and radiological verification of BBB disruption is often needed during clinical procedures, often after the delivery of chemotherapeutic drugs [11, 12].

The osmotic disruption of the BBB is affected by a number of factors, Table 1 [13]. Variations in BBB disruption could have a profound impact on the regional delivery of chemotherapeutic drugs. Inadequate disruption could lead to failure of treatment, while severe disruption could lead to seizures or even fatal brain edema [11]. The ability to quantify drug and tracer concentrations in vivo using the method of optical pharmacokinetics, a variation of diffuse reflectance spectroscopy, leads to the possibility of detecting and quantifying blood–brain-barrier disruption in vivo in real-time [14–18]. Optical detection of drug concentrations requires the drug to have a chromophore absorption band whose spectrum is sufficiently distinct from those of oxyhemoglobin and deoxyhemoglobin. The absorbance spectrum of Evan's Blue lends well to such

**Table 1** Factors affecting hyperosmotic disruption of the blood brain barrier

Physiological:	Pathological states:
Anatomical: regional [34]	Blood–tumor barrier [35]
Hypercapnia [36]	Inflammation [37]
Blood pressure [38]	Diseases states, e.g., multiple sclerosis [39, 40]
Temperature [28]	Seizure [41, 42]
Blood flow [19]	Ischemia [43]
Pharmacological:	Largely uninvestigated:
Type of agent: mannitol versus arabinose [31]	Depth of anesthesia
	Species susceptibility
Steroids [44]	Assessment:
Mg <sup>++</sup> , Ca <sup>++</sup> [45, 46]	Time elapsed [10, 47]
Anesthetic drugs [13, 29]	Criteria [50]
Nitric oxide [48, 49]	

measurements. Evan's Blue (MW 980 Da) is a water-soluble dye that is traditionally used to demonstrate the opening of the BBB.

Our hypothesis was that it is feasible to track disruption of the BBB by monitoring tissue concentrations of Evan's Blue. Furthermore, variations in BBB disruption will have a profound impact on the magnitude and rate of Evan's Blue uptake.

## Methods

We tested our hypothesis in anesthetized New Zealand white rabbits, which have a primate-like separation of internal (ICA) and external carotid arteries and are sufficiently large to safely permit required instrumentation and monitor the physiologic parameters. The protocol was approved by the Institutional Animal Care and Use Committee. Animals had free access to food and water prior to experiments. In the past, we had observed great variability in BBB disruption after intracarotid mannitol injection in our rabbit model [19]. Subsequently, we eliminated the potential confounders, such as the empirical use of steroids, varying depth of anesthesia, temperature, method of injection, and preparation of mannitol. We took meticulous care in isolating the ICA and standardizing the dose response characteristics in each animal experiment [20]. Yet, the variability persisted in the preliminary studies, Fig. 2a–c.

Surgical preparation was undertaken under intramuscular ketamine sedation with intravenous propofol anesthesia, which was supplemented by infiltration of the incision sites with a long acting local anesthetic agent, bupivacaine. The preparation included: tracheotomy for mechanical ventilation aimed at an end tidal CO<sub>2</sub> of 30–40 mmHg, femoral

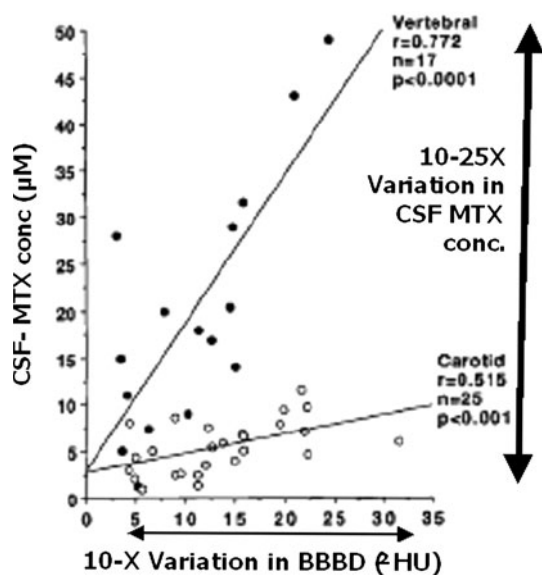


**Fig. 1** Variation in blood brain barrier disruption (BBBD) by intraarterial mannitol 3–11 ml/s for 30 s in human subjects. There is a 10× variation in the degree of barrier opening as judged by CT imaging, Hounsfield Units ( $\Delta$ HU). There is also a 10–25× variation in CSF concentrations of methotrexate (MTX) that is more pronounced with vertebral injections than with carotid injections [8]. Reproduced with the permission of the journal

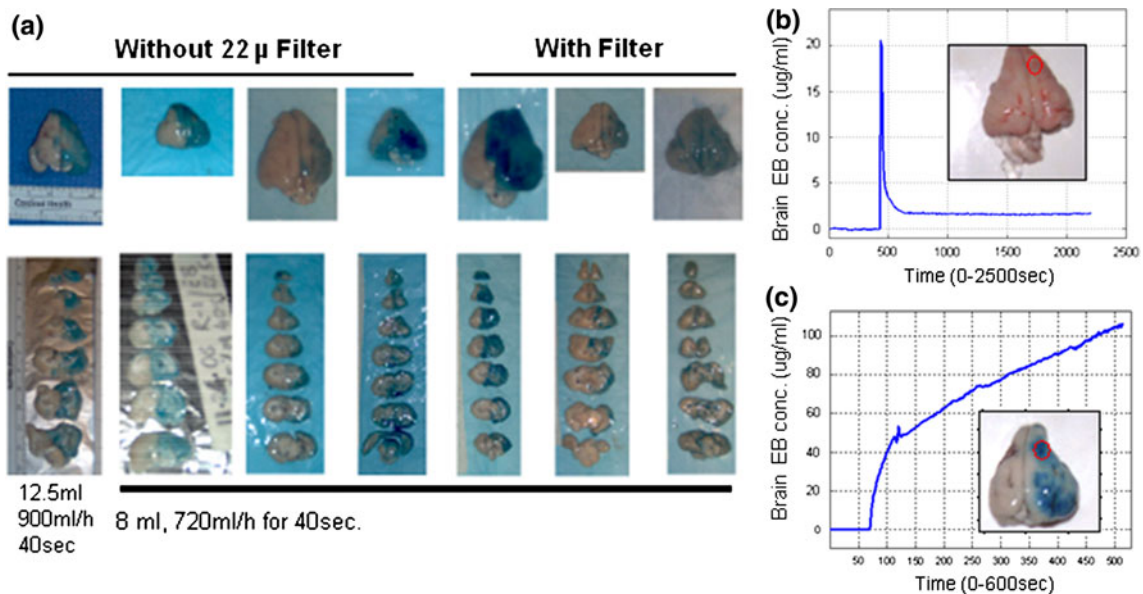


**Fig. 2** **a** Preliminary observations regarding the variability in BBBD in rabbits with intracarotid injection of 8 ml of 25% mannitol. Interposition of filter did not affect the variation in the staining pattern in seven animals. The experiments repeated in another 12 rabbits showed similar results who received 50 mg/kg of Evan's Blue. **b** Time–concentration profile of minimal Evan's Blue tissue uptake in

one animal contrasts sharply with the rapid and progressive increase in Evan's Blue concentrations in another. **c** Autopsy brain tissue pictures, *inset* to the *right* of each graph, show the Evan's Blue staining. The optical measurements were made at the *center* of the *red circle*

and selective ICA catheterizations, skull screws for monitoring electrocerebral activity, bilateral placement of laser Doppler probes and a small craniotomy for placement of the OP fiberoptic probe to measure tissue Evan's Blue concentration over the parietal cortex. EEG activity was carefully monitored and propofol infusion was targeted to low-frequency, high-amplitude activity of about 100–200  $\mu$ V, interspersed with low-amplitude, high-frequency activity. The esophageal temperature was maintained at 36–37°C. Intravenous fluids were administered at a rate of 20 ml/kg/h and consisted of a mixture of lactated Ringer's solution, 5% albumin, and 5% dextrose in a ratio of 3:1:1. Oxygen saturation and EEG activity were monitored in real-time. This experimental protocol ensures stable hemodynamics, and the preparation can withstand fairly severe hemodynamic stresses [21].

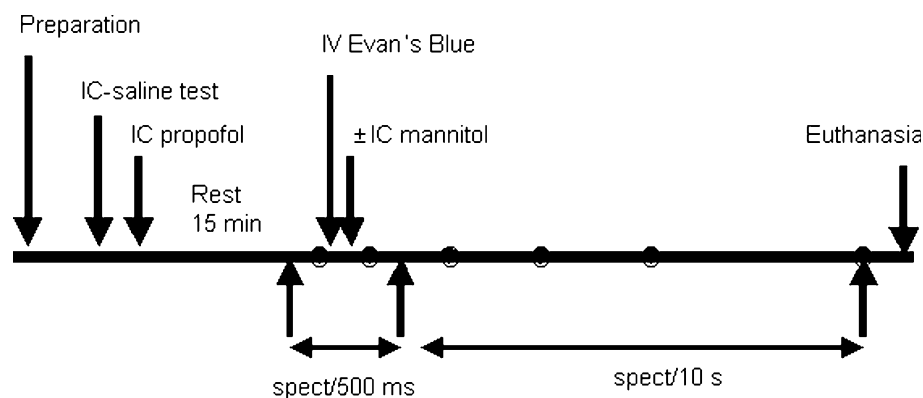
Considerable precautions were taken to ensure correct isolation of the ICA, which exhibits considerable variation in the anatomy for this species [22]. Therefore, it is necessary to correctly isolate the artery and establish a dose response prior to experimental drug delivery. Two operators with sufficient experience confirmed the origin of the ICA. On identification, the ICA was isolated from all other arterial branches using an atraumatic arterial clip. Next, a 0.5-ml saline bolus was injected to demonstrate a blanching of the retinal vessels, thus verifying catheter placement [23]. Later, the animal was secured to the stereotactic frame, and laser Doppler probes were placed on the skull.

Then 0.25 ml of saline was injected to see if the vessel was correctly isolated, causing an abrupt decrease in blood flow, as sensed by both of the laser Doppler probes [20]. Finally, 0.4 ml of propofol was injected, producing a short period of electrocerebral quiescence for 5–10 s, if the saline injection produced a questionable decrease in laser Doppler blood flow, which is consistent with an effective delivery of 2 mg of the drug [24]. Collectively all these tests assured the correct isolation of the artery in all animals.

Optical pharmacokinetics (OP), a variation of diffuse reflectance spectroscopy, is a non-invasive, real-time method that was developed to non-invasively measure concentrations of chromophores in turbid media [24]. Briefly, as implemented here, a pulsed xenon-arc lamp is used as a broadband illumination light source. A fiber optic probe, with separate source and detector fibers, with its tip placed gently in direct contact with the dura, is used to collect absorption spectra of Evan's Blue over time from the tissue beneath. Determination of the Evan's Blue concentration is accomplished by using a modified Beer's Law to derive the total absorption coefficient change, from spectra measured before and after Evan's Blue administration. The tissue volume that is sampled is approximately 3  $\times$  3 mm in area, to a depth of approximately 3 mm.

The experimental preparation was allowed to recover for 15 min. Over the fronto-parietal cortex, a small area of the skull flap was removed, and the optical fiber probe was

**Fig. 3** Experimental protocol showing time line of interventions and the collection of data



placed in contact with the dura. Wetting the surface with saline provided reliable optical contact between the fiber tip and the dura. Figure 3 shows the sequence of the experiment.

Measurements before the Evan's Blue dye administration, baseline optical data, were collected for 1 min at a rate of 12 spectra/min. For each animal the number of integrated light pulses was adjusted to obtain adequate optical signal in the 450–900 nm range. (A single spectral measurement takes 100–300 ms.) After acquisition of the baseline spectra, the rate of data acquisition was increased to obtain 300 spectra every 0.5 s. Concurrent with the start of the higher data acquisition rate, Evan's Blue (6.5 mg/kg) was injected intravenously as a 0.2% solution at a rate of 6 ml/min. Approximately 30 s after completing the infusion (approximately 1 min after start of Evan's Blue infusion), intraarterial mannitol 25% was infused at a rate of 8 ml/40 s. The tissue concentration of Evan's Blue was monitored over the next hour, acquiring spectra every 10 s. Overall, 612 measurements were obtained in each animal over a period of approximately 60 min. The slight variability was due to the differences in the duration of the light pulse necessary to obtain an optimum spectrum that varied between animals.

Hemodynamic data, blood pressure, and EEG activity were recorded at a frequency of 200/s. Representative data were analyzed at six time points: (i) baseline; (ii–vi) 1, 5, 15, 30 and 60 min after mannitol injection. Heparinized blood samples, for the determination of plasma Evan's Blue concentrations, were taken before and immediately after mannitol injection, then 5, 15, 30 and 60 min thereafter. To determine plasma Evan's Blue concentrations, a 1-ml sample of arterial blood was centrifuged at 12,000 rpm for 15 min, the supernatant was diluted in formamide (1:10,000), and the concentration was optically measured by a spectrophotometer in batches of up to 48 samples per run. Paired samples were analyzed to assess the consistency of measurements. A control Evan's Blue dilution curve was determined to convert the absorbance values to plasma

Evan's Blue concentrations for each run. The animals were euthanized 60 min after injection of mannitol, and brain tissue was harvested for postmortem examination for each animal. *Data analysis:* As indicated above, the data were collected at six time points for each challenge: baseline, 1 min after mannitol or 2 min after Evan's Blue, 5, 15, 30 and 60 min after mannitol. Within each group (mannitol and control), data at the six time points were analyzed by repeated measures ANOVA. Across the groups (control and mannitol), data were analyzed by factorial ANOVA. A Bonferroni–Dunn post-hoc test was used for multiple comparisons. A *P* value of <0.0033 was deemed good for repeat measurements, while a *P* value of <0.05 was considered significant between the two groups.

## Results

Twenty-three New Zealand white rabbits were randomly assigned to two groups: control ( $n = 13$ ) and mannitol ( $n = 10$ ) groups. Persistent bleeding in one case, and noisy data due to movements of the probe relative to the head, resulted in data artifacts that prevented further analysis for two animals in the mannitol group and one in the control group. Therefore, data from 11 controls and 9 mannitol treated animals was available for the final analysis.

The hemodynamic and cerebral vascular effects of mannitol injection were assessed as follows: the baseline weight, heart rate, mean arterial pressure, end-tidal carbon dioxide concentrations, respiratory rate, temperature and oxygen saturation were comparable in the two groups. Most physiological parameters remained stable during the study. There was an increase in CBF lasting for 5 min with the injection of mannitol, which is typical. As expected, injection of Evan's Blue perturbed measurement of the oxygen saturation due to the interference of the dye with pulse oximeter measurements (see Table 2). The saturation decreased nearly to the lowest level recordable by the oximeter (70%) after Evan's Blue injection.

**Table 2** Physiological changes in control (n = 11) and mannitol (n = 9) treatment groups

	Treatment	Baseline	1 min	5 min	15 min	30 min	60 min
Esophageal temperature (°C)	Control	36.8 ± 1.5	36.7 ± 1.5	36.5 ± 1.4	36.6 ± 1.3	36.8 ± 1.1	37.0 ± 0.9
	Mannitol	36.4 ± 0.6	36.5 ± 0.6	36.4 ± 0.5	36.5 ± 0.6	37.0 ± 0.7	37.0 ± 0.7
ETCO <sub>2</sub> (mmHg)	Control	35 ± 9	36 ± 9	36 ± 9	36 ± 9	35 ± 9	36 ± 9
	Mannitol	37 ± 2	33 ± 3	32 ± 3	33 ± 3	33 ± 3	32 ± 3
Respiration rate (bpm)	Control	58 ± 13	58 ± 13	58 ± 13	58 ± 13	58 ± 13	58 ± 13
	Mannitol	53 ± 10	53 ± 10	53 ± 10	53 ± 10	53 ± 10	53 ± 10
Heart rate (beats/min)	Control	255 ± 22	264 ± 24	262 ± 23	268 ± 18	270 ± 21 <sup>a</sup>	275 ± 21 <sup>a</sup>
	Mannitol	263 ± 21	261 ± 18	262 ± 17	280 ± 30	276 ± 20	285 ± 17 <sup>a</sup>
LDI (%change)	Control	100 ± 0	95 ± 12 <sup>c</sup>	100 ± 12 <sup>c</sup>	102 ± 15	109 ± 26	108 ± 22 <sup>b</sup>
	Mannitol	100 ± 0	151 ± 74	169 ± 66 <sup>a</sup>	120 ± 36	122 ± 38	115 ± 34 <sup>b</sup>
LDC (%change)	Control	100 ± 0	99 ± 13 <sup>c</sup>	89 ± 47	109 ± 14	120 ± 29	122 ± 31
	Mannitol	100 ± 0	134 ± 54	90 ± 62	111 ± 29	107 ± 27	108 ± 29
MAP (mmHg)	Control	88 ± 11	82 ± 12	82 ± 9	81 ± 9	81 ± 8	84 ± 10
	Mannitol	87 ± 8	83 ± 23	85 ± 22	88 ± 10	88 ± 11	81 ± 23
SO <sub>2</sub>	Control	93 ± 6	70 ± 1 <sup>a</sup>	71 ± 2 <sup>a</sup>	72 ± 2 <sup>a</sup>	74 ± 5 <sup>a</sup>	74 ± 5 <sup>a</sup>
	Mannitol	91 ± 9	72 ± 3 <sup>a</sup>	72 ± 3 <sup>a</sup>	72 ± 4 <sup>a</sup>	74 ± 5 <sup>a</sup>	75 ± 6 <sup>a</sup>

The data is presented as mean ± 1 standard deviations

*bpm* Breaths per minute, *LDI* laser Doppler flow ipsilateral cerebral hemisphere, *LDC* laser Doppler flow contralateral cerebral hemisphere, *SaO<sub>2</sub>* arterial blood oxygen saturation

<sup>a</sup> Different from base; <sup>b</sup> different from 1 min; <sup>c</sup> different between treatments

#### Plasma concentrations

The injection of Evan's Blue led to a similar initial increase in plasma concentrations of the dye for both groups. However, there was significant difference in plasma concentrations of Evan's Blue between the control and the mannitol groups 5–60 min after the injection of the dye as seen in Fig. 4a.

#### Tissue concentrations

Concentrations of Evan's Blue in brain tissue increased progressively in the mannitol group over time, Fig. 4b. The tissue concentrations of Evan's Blue after the disruption of the BBB were 6 times the control values at the end of 60 min. A small progressive rise in tissue concentrations of Evan's Blue was also seen in the control group.

#### Brain: plasma Evan's Blue ratio

The calculated partition ratio between brain and plasma Evan's Blue concentrations showed a progressive increase over time as seen in Fig. 4c. Large variation was seen in the tissue Evan's Blue concentrations after intraarterial mannitol (2.9–76.18 µg/ml), and the range of the brain:plasma partition coefficient (0.012–0.46) at 60 min was larger than the range of the corresponding values in the control group: (1.77–8.59 µg/ml). Figures 5 and 6 illustrate

the two extreme examples of EB uptake after BBBD in this study. The peak EB concentration in Fig. 6 was 76.18 µg/ml that was almost 20-fold higher than in peak concentration in Fig. 5, 3.5 µg/ml.

#### Discussion

Disruption of the BBB is a critical step in the delivery of a variety of chemotherapeutic drugs. This study shows that it is possible to track tissue concentration of a marker for BBB disruption (Evan's Blue), in real-time using optical pharmacokinetics. The major finding of this study was that BBB can be disrupted by intraarterial mannitol; however, the severity of disruption is inconsistent. Mannitol had been widely used in clinical setting, and we decided to investigate this application first. It is generally accepted that the inconsistency of disruption is a consequence of physiological variation, and a variety of other factors, Table 1. Although this finding by itself is not novel, to our best knowledge, this is the first report describing the use of tissue noninvasive optical technology to track BBB disruption.

The current clinical method of BBB disruption uses angiographic determination of the rate of mannitol injection. Intraarterial mannitol is injected at a rate that is the minimal rate for the contrast to reflux into the feeding artery [10]. This rate of injection varies from 3–11 ml/s. To

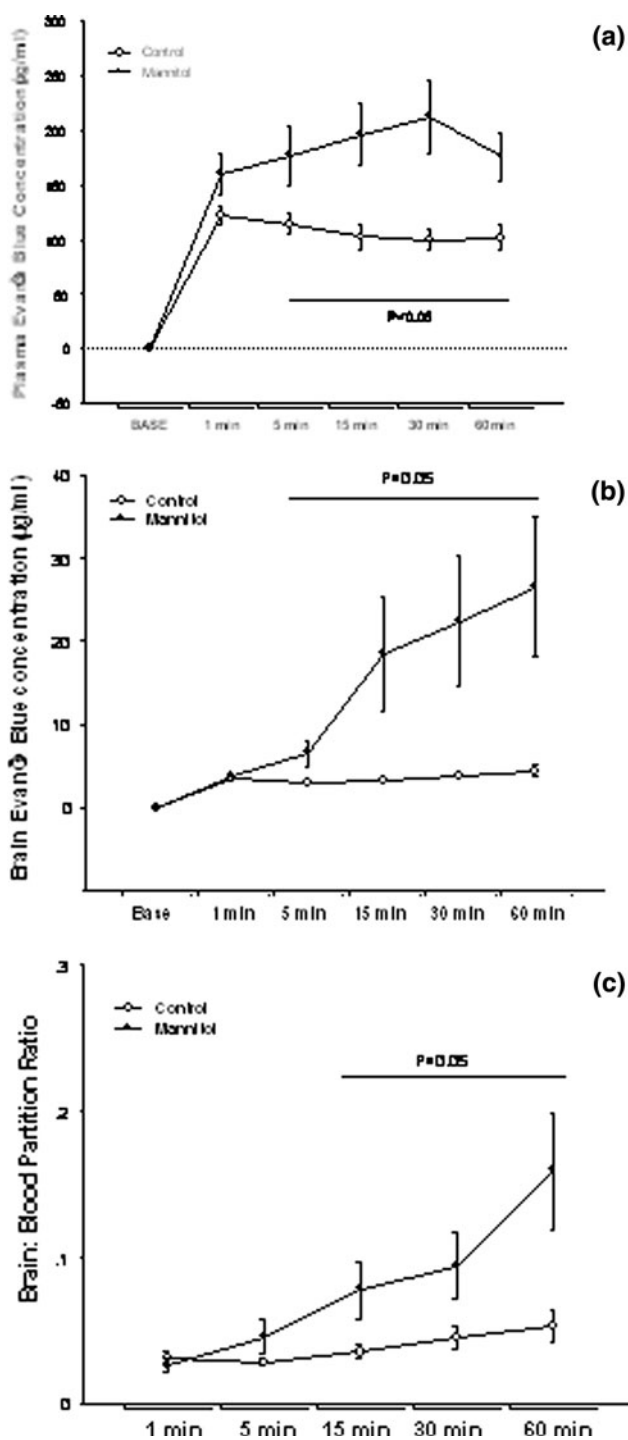


**Fig. 4** Change in brain tissue and plasma concentration over time in control (n = 11) and mannitol (n = 9) treated animals. The observations were recorded at baseline (base) and at five other time points as shown in the ordinate. The abscissa shows the changes in **a** plasma Evan's Blue concentrations (µg/ml), **b** brain Evan's Blue concentration (µg/ml) and **c** brain: plasma partition ratio of Evan's Blue

effectively disrupt the BBB the rate must be maintained for at least 30 s. The volume of mannitol required in human subjects varies from 90 to 330 ml [8]. In the rabbit a

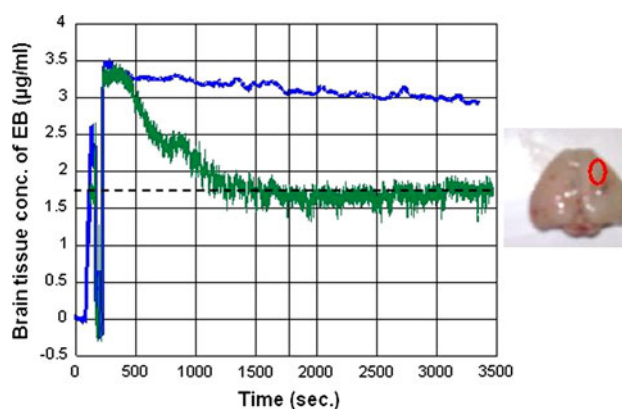


**Fig. 5** The least uptake of EB after disruption of the BBB by intraarterial mannitol in this study. In this case, the injection of mannitol resulted in a severe reduction in blood flow with a significant hyperemic response. The ordinate shows the time in seconds while the abscissa shows the brain tissue Evan's Blue concentration in µg/ml. The concentration of Evan's Blue does not change over time suggesting if the BBB opened at anytime, it was very transient. The peak EB concentrations were 3.5 and 2.9 µg/ml at the end of 60 min. On autopsy, there is little tissue staining with Evan's Blue. The oval represents the site of optical measurements in the center. Dashed line indicate baseline blood flow

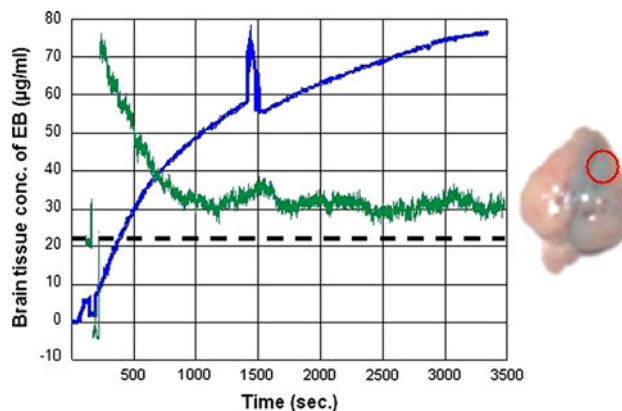


**Fig. 6** The extreme example of uptake of EB after BBB disruption in this study. There was progressive tissue uptake of Evan's Blue after the disruption of the BBB (blue line). Relative changes in CBF are shown in green. The baseline blood flow is shown as black dashed line. Injection of mannitol decreased CBF to near zero after which there was a significant hyperemic response and blood flow remained persistently high over the next hour, black dashed line. The ordinate shows the time in seconds while the abscissa shows the brain tissue Evan's Blue concentration in µg/ml (blue). There is an artifact due to transient movement of the probe at 1,350 s. The concentrations at the end of 60 min were 76.18 µg/ml. Postmortem specimen on the right shows the Evan's Blue staining. The center of the red circle indicates the site of optical measurement

volume of 8 ml/40 s has been recommended for disrupting the BBB [19, 23]. While we did not undertake angiographic measurements, we observed that the CBF as measured by laser Doppler transiently decreased to near zero during mannitol infusion (see Figs. 5, 6), suggesting

that the rate of mannitol infusion was sufficient to transiently overwhelm the CBF in our model by displacing blood.

Immediately after mannitol injection, we observed a rebound increase in blood flow. The hyperemic response lasted for 5–10 min. We did not observe any consistent change in blood pressure or in the heart rate. In both the mannitol and the control groups, the heart rate showed a progressive, though statistically insignificant, increase over time. Hypertension, bradycardia and arrhythmias have been reported during clinical disruption of the BBB with intraarterial mannitol. We occasionally observed a hypertensive response, but overall hemodynamic changes were not statistically significant. We frequently observed attenuation of EEG activity to the point of silence, often followed by a persistent loss of high frequency EEG activity after mannitol injection. The use of EEG to detect BBB disruption needs to be assessed in future studies.

Evan's Blue is a classical marker of BBB disruption. The traditional dose of plasma Evan's Blue used for determining BBB disruption in rabbits can be as high as 25–90 mg/kg which produces intense blue coloration of the brain tissue that can be visually assessed [25, 26]. However, this dose of Evan's Blue does not reflect the subtle concentrations of chemotherapeutic drugs and can overwhelm optical measurements. We therefore employed a much smaller dose of Evan's Blue, 6.5 mg/kg, which was sufficient to be detected by the OP method, yet remained discernable to the eye for the post-mortem tissue, Fig. 6.

The plasma Evan's Blue concentrations were comparable 1 min after mannitol injection but showed two distinct trends. Although the plasma concentration remained stable in each group, over time a significant difference emerged between mannitol treated and the control group. Since Evan's Blue binds to plasma proteins and its clearance from the central compartment is slow due to a slow uptake by tissues, plasma Evan's Blue concentrations provide a measure of plasma volume. We suspect that the increase in concentrations of Evan's Blue over time could be due to diuresis by mannitol and a contraction of the plasma volume.

Optically measured brain tissue concentrations of Evan's Blue increased progressively after mannitol injection by a factor 2 at 5 min, increasing to a factor 5 at 1 h. This indicates a progressive tissue uptake of Evan's Blue after BBB disruption. A small (25%) increase in tissue concentration of Evan's Blue was evident in the controls and could reflect non-specific uptake of Evan's Blue at the site of optical probe placement. Some injury in the preparation is likely to occur when the skull flap is removed. The removal of the bone flap is often complicated by its adherence to the dura, as well as the potential injury that could occur from the vibrations of the surgical drill.

Although optical measurements are generally taken through the inner table of the skull, in this particular study the measurements were made through the dura to improve the signal-to-noise ratio, which was initially thought to be necessary with the decrease in the dose of Evan's Blue. Due to the trend of plasma concentrations to increase in the mannitol group and decrease in the control group, we also assessed the brain:plasma Evan's Blue partition coefficient. The tissue partition coefficient also progressively increased over time and was three times higher in the mannitol group.

The results that show a progressive increase in Evan's Blue tissue concentration suggest that the BBB remains open for at least an hour after mannitol injection. In human clinical studies the peak CSF concentration did not occur until 8–10 h after mannitol injection. The increase in CSF concentrations was believed to be due to the release of the drug from the brain parenchyma into the CSF rather than the sustained opening of the BBB [8]. It is generally believed that mannitol only transiently disrupts the BBB. This, however, may not always be the case. For example, in rodents the BBB remained opened for 6 h after mannitol injection [10].

The BBB is often assumed to be a simple tissue membrane rather than a complex regulatory system. Considering the dynamic nature and the multitude of complex processes that determine the transport of substances across the barrier, it is a reasonable assumption that a number of factors affect the duration and the degree of BBB disruption. The ability to optically track brain-tissue tracer concentrations can help us understand these factors. For example, in Figs. 5 and 6, we see two different patterns of tracer uptake after BBB disruption. In one case the tissue concentration of Evan's Blue progressively increases and follows a saturation pattern, whereas, in the other case, there is minimal early uptake of the Evan's Blue, but the concentrations do not increase over time. This suggests that in the first case, the BBB remained open for at least an hour while in the other case, it opened only transiently, if at all. Furthermore, we observed a wide range of tissue Evan's Blue concentrations (and brain: plasma partition coefficient) after BBB disruption, reflecting the different degrees of BBB disruption with intraarterial mannitol.

Variability of BBB disruption has been attributed to a number of factors. Regional variations in BBB disruption are often seen in different arterial distributions; e.g., a close examination of the data in Fig. 1 reveals that for a given degree of disruption of the BBB, the CSF concentrations of methotrexate were higher with vertebral artery injection when compared to carotid injection [8]. The difference could be due to the increased transport across the choroid plexuses or to a more prolonged BBB disruption with vertebral artery injections. It is generally believed that the BBB of malignant tumors is more sensitive to disruption,

or is already disrupted for angiogenic microvessels [27]. Hypothermia [28], hypercapnia [13] and background anesthesia also affect the hypertonic disruption of the BBB, Table 1. While hypothermia and hypercapnia protect the BBB, hyperthermia and hypocapnia do not. Volatile anesthetic agents, such as methoxyflurane, sometimes isoflurane, and narcotics attenuate BBBD, while anesthetic agents, like ketamine and thiopental, augment the disruption [29, 30]. Intravenous propofol does not adversely affect BBBD [10].

Over the years a number of alternatives to mannitol have been proposed, and some of them seem superior to mannitol in preclinical testing. They include osmotic agents like arabinose [31], contrast agents like Optison [32], and bradykinin analogues like RMP-7 (Cereport) [3]. [However, none of them has been accepted in clinical practice. Optical measurements could help compare the efficacy of these agents with that of mannitol. Current intraarterial chemotherapy regimens for brain tumors use a fixed angiographically determined dose of mannitol and predetermined doses of chemotherapeutic drugs. The disruption of the BBB is usually assessed by injection of contrast agents within 5–90 min of mannitol injection [8, 10–12]. Most contrast agents used for X-ray or magnetic resonance imaging have potentially neurotoxic effects. As many as 25% of patients who undergo BBB disruption present with focal seizures that are, in part, due to the use of contrast for imaging purposes [11]. Overall there are concerns regarding the safety and efficacy of BBB disruption [10]. In experienced hands, the procedure is safe and effective. Although effort has been made to improve the consistency of the technique, it is still available in only a handful of centers.

Translating our results to human subjects is theoretically possible by the use of clinical near-infrared spectroscopic devices with tracers like indocyanine green [29]. NIRS optical grids with combinations of several emitter and receiving fibers that can monitor changes in tissue spectrum over large cortical zones could provide a better quantification of BBB disruption [33]. Given the larger scale of human heads, such devices can be used through the intact scalp and skull. There are many advantages in developing optical technologies to monitor BBB disruption. Optical feedback during BBB disruption could help to determine if there was any need to disrupt the barrier, as the blood:tumor barrier might already be permeable in a given patient, to determine the dose of mannitol, alter the dose of chemotherapeutic drugs based on the degree of BBB disruption, predict complications, and avoid the use of radiocontrast agents.

In conclusion, we show the feasibility of real-time monitoring of BBB disruption by quantifying the brain tissue tracer concentrations of Evan's Blue by the method of optical pharmacokinetics. Optical measurements

revealed that after intraarterial mannitol injection there was a progressive increase in tissue Evan's Blue concentrations and an increase in the brain:plasma Evan's Blue partition concentrations over time. These results suggest that, in the rabbit model, the BBB remains disrupted for an hour after intraarterial mannitol. The degree and duration of BBB disruption with intraarterial mannitol was also shown to be highly variable, as evidenced by a wide range of tissue Evan's Blue concentrations and brain:plasma partition coefficient. The variation was readily monitored by the optical measurements. In pre-clinical studies, optical quantification of BBB disruption could advance the understanding of drug delivery to the brain; and, during clinical procedures, feedback control of BBB disruption could increase the safety and efficacy of intraarterial mannitol, facilitating better control of delivery of chemotherapy agents to brain tissues.

**Acknowledgments** Funding This work was supported in part by the NIH/NCI R01-CA-12500, (SJ) R01-CA82104; U54-CA104677 (IB).

## References

1. Neuwelt E, Abbott NJ, Abrey L et al (2008) Strategies to advance translational research into brain barriers. *Lancet Neurol* 7:84–96
2. Nagaraja TN, Keenan KA, Fenstermacher JD, Knight RA (2008) Acute leakage patterns of fluorescent plasma flow markers after transient focal cerebral ischemia suggest large openings in blood–brain barrier. *Microcirculation* 15:1–14
3. Black KL, Cloughesy T, Huang SC et al (1997) Intracarotid infusion of RMP-7, a bradykinin analog, and transport of gallium-68 ethylenediamine tetraacetic acid into human gliomas. *J Neurosurg* 86:603–609
4. Bhattacharjee AK, Kondoh T, Nagashima T et al (2001) Quantitative analysis of papaverine-mediated blood–brain barrier disruption in rats. *Biochem Biophys Res Commun* 289:548–552
5. Cloughesy TF, Black KL, Gobin YP et al (1999) Intra-arterial Cereport (RMP-7) and carboplatin: a dose escalation study for recurrent malignant gliomas. *Neurosurgery* 44:270–278 (discussion 278–279)
6. Lee HJ, Zhang Y, Pardridge WM (2002) Blood–brain barrier disruption following the internal carotid arterial perfusion of alkyl glycerols. *J Drug Target* 10:463–467
7. Neufeld GR (1971) Computation of transit time distributions using sampled data Laplace transforms. *J Appl Physiol* 31:148–153
8. Zylber-Katz E, Gomori JM, Schwartz A et al (2000) Pharmacokinetics of methotrexate in cerebrospinal fluid and serum after osmotic blood–brain barrier disruption in patients with brain lymphoma. *Clin Pharmacol Ther* 67:631–641
9. Doolittle ND, Miner ME, Hall WA et al (2000) Safety and efficacy of a multicenter study using intraarterial chemotherapy in conjunction with osmotic opening of the blood–brain barrier for the treatment of patients with malignant brain tumors. *Cancer* 88:637–647
10. Bellavance MA, Blanchette M, Fortin D (2008) Recent advances in blood-brain barrier disruption as a CNS delivery strategy. *AAPS J* 10:166–177

11. Marchi N, Angelov L, Masaryk T et al (2007) Seizure-promoting effect of blood–brain barrier disruption. *Epilepsia* 48:732–742
12. Elkassabany NM, Bhatia J, Deogaonkar A et al (2008) Perioperative complications of blood brain barrier disruption under general anesthesia: a retrospective review. *J Neurosurg Anesthesiol* 20:45–48
13. Rensen LG, Pagel MA, McCormick CI et al (1999) The influence of anesthetic choice, PaCO<sub>2</sub>, and other factors on osmotic blood–brain barrier disruption in rats with brain tumor xenografts. *Anesth Analg* 88:559–567
14. Mourant JR, Johnson TM, Los G, Bigio IJ (1999) Non-invasive measurement of chemotherapy drug concentrations in tissue: preliminary demonstrations of in vivo measurements. *Phys Med Biol* 44:1397–1417
15. Bigio IJ, Mourant JR (1997) Ultraviolet and visible spectroscopies for tissue diagnostics: fluorescence spectroscopy and elastic-scattering spectroscopy. *Phys Med Biol* 42:803–814
16. Bigio IJ, Mourant JR, Los G (1999) Noninvasive, in situ measurement of drug concentrations in tissue using optical spectroscopy. *J Gravit Physiol* 6:P173–P175
17. Reif R, Wang M, Joshi S et al (2007) Optical method for real-time monitoring of drug concentrations facilitates the development of novel methods for drug delivery to brain tissue. *J Biomed Opt* 12:034036
18. Kanick SC, Eiseman JL, Joseph E et al (2007) Noninvasive and nondestructive optical spectroscopic measurement of motexafin gadolinium in mouse tissues: comparison to high-performance liquid chromatography. *J Photochem Photobiol B* 88:90–104
19. Wang M, Etu J, Joshi S (2007) Enhanced disruption of the blood brain barrier by intracarotid mannitol injection during transient cerebral hypoperfusion in rabbits. *J Neurosurg Anesthesiol* 19:249–256
20. Joshi S, Wang M, Hartl R (2004) Retinal discoloration test. *J Cereb Blood Flow Metab* 24:305–308
21. Joshi S, Wang M, Nishanian EV, Emerson RG (2004) Electro-cerebral silence by intracarotid anesthetics does not affect early hyperemia after transient cerebral ischemia in rabbits. *Anesth Analg* 98:1454–1459 (table of contents)
22. Lee JS, Hamilton MG, Zabramski JM (1994) Variations in the anatomy of the rabbit cervical carotid artery. *Stroke* 25:501–503
23. Perkins BA, Strausbaugh LJ (1983) Effect of mannitol infusions into the internal carotid artery on entry of two antibiotics into the cerebrospinal fluid and brains of normal rabbits. *Antimicrob Agents Chemother* 24:339–342
24. Wang M, Joshi S (2002) Comparison of intravenous and intracarotid propofol for electrical silence on EEG. *J Neurosurg Anesthesiol* 14:333
25. Strausbaugh LJ (1987) Intracarotid infusions of protamine sulfate disrupt the blood–brain barrier of rabbits. *Brain Res* 409:221–226
26. Chen X, Gawryluk JW, Wagener JF et al (2008) Caffeine blocks disruption of blood brain barrier in a rabbit model of Alzheimer's disease. *J Neuroinflamm* 5:12
27. Provenzale JM, Mukundan S, Dewhirst M (2005) The role of blood–brain barrier permeability in brain tumor imaging and therapeutics. *AJR Am J Roentgenol* 185:763–767
28. Chi OZ, Liu X, Weiss HR (2001) Effects of mild hypothermia on blood–brain barrier disruption during isoflurane or pentobarbital anesthesia. *Anesthesiology* 95:933–938
29. Gumerlock MK, Neuwelt EA (1990) The effects of anesthesia on osmotic blood–brain barrier disruption. *Neurosurgery* 26:268–277
30. Chi OZ, Chun TW, Liu X, Weiss HR (1998) The effects of pentobarbital on blood–brain barrier disruption caused by intracarotid injection of hyperosmolar mannitol in rats. *Anesth Analg* 86:1230–1235
31. Bullard DE, Bourdon M, Bigner DD (1984) Comparison of various methods for delivering radiolabeled monoclonal antibody to normal rat brain. *J Neurosurg* 61:901–911
32. Mychaskiw G II, Badr AE, Tibbs R et al (2000) Optison (FS069) disrupts the blood–brain barrier in rats. *Anesth Analg* 91:798–803
33. Wolf M, Ferrari M, Quaresima V (2007) Progress of near-infrared spectroscopy and topography for brain and muscle clinical applications. *J Biomed Opt* 12:062104
34. Ueno M (2007) Molecular anatomy of the brain endothelial barrier: an overview of the distributional features. *Curr Med Chem* 14:1199–1206
35. Riina HA, Fraser JF, Fralin S et al (2009) Superselective intra-arterial cerebral infusion of bevacizumab: a revival of interventional neuro-oncology for malignant glioma. *J Exp Ther Oncol* 8:145–150
36. Baumbach GL, Mayhan WG, Heistad DD (1986) Protection of the blood–brain barrier by hypercapnia during acute hypertension. *Am J Physiol* 251:H282–H287
37. Ballabh P, Braun A, Nedergaard M (2004) The blood–brain barrier: an overview: structure, regulation, and clinical implications. *Neurobiol Dis* 16:1–13
38. Al-Sarraf H, Ghaedi F, Redzic Z (2007) Time course of hyperosmolar opening of the blood–brain and blood–CSF barriers in spontaneously hypertensive rats. *J Vasc Res* 44:99–109
39. van Horssen J, Brink BP, de Vries HE et al (2007) The blood–brain barrier in cortical multiple sclerosis lesions. *J Neuropathol Exp Neurol* 66:321–328
40. Soon D, Tozer DJ, Altmann DR et al (2007) Quantification of subtle blood–brain barrier disruption in non-enhancing lesions in multiple sclerosis: a study of disease and lesion subtypes. *Mult Scler* 13:884–894
41. Ruda R, Trevisan E, Soffietti R (2010) Epilepsy and brain tumors. *Curr Opin Oncol* 22(6):611–620
42. Kalayci R, Kaya M, Ahishali B et al (2006) Long-term L-NAME treatment potentiates the blood–brain barrier disruption during pentylenetetrazole-induced seizures in rats. *Life Sci* 79:16–20
43. Brown RC, Davis TP (2002) Calcium modulation of adherens and tight junction function: a potential mechanism for blood–brain barrier disruption after stroke. *Stroke* 33:1706–1711
44. Neuwelt EA, Barnett PA, Ramsey FL et al (1993) Dexamethasone decreases the delivery of tumor-specific monoclonal antibody to both intracerebral and subcutaneous tumor xenografts. *Neurosurgery* 33:478–484 (discussion 484)
45. Euser AG, Bullinger L, Cipolla MJ (2008) Magnesium sulphate treatment decreases blood–brain barrier permeability during acute hypertension in pregnant rats. *Exp Physiol* 93:254–261
46. Bhattacharjee AK, Nagashima T, Kondoh T, Tamaki N (2001) The effects of the Na(+)/Ca(++) exchange blocker on osmotic blood–brain barrier disruption. *Brain Res* 900:157–162
47. Siegal T, Rubinstein R, Bokstein F et al (2000) In vivo assessment of the window of barrier opening after osmotic blood–brain barrier disruption in humans. *J Neurosurg* 92:599–605
48. Boje KM, Lakhman SS (2000) Nitric oxide redox species exert differential permeability effects on the blood–brain barrier. *J Pharmacol Exp Ther* 293:545–550
49. Boje KM (1996) Inhibition of nitric oxide synthase attenuates blood–brain barrier disruption during experimental meningitis. *Brain Res* 720:75–83
50. Brown RC, Egleton RD, Davis TP (2004) Mannitol opening of the blood–brain barrier: regional variation in the permeability of sucrose, but not 86Rb+ or albumin. *Brain Res* 1014:221–227